Physica 26D (1987) 181–192
North-Holland, Amsterdam

AN OBSTRUCTION METHOD FOR THE DESTRUCTION OF INVARIANT CURVES

Arturo OLVERA and Carles SIMÓ
Departament d'Equacions Funcionals, Facultat de Matemàtiques, Universitat de Barcelona, Gran Via 585, Barcelona 08007, Spain

Received 4 March 1986
Revised manuscript received 26 August 1986

An important point in a conservative dynamical system which is a parameter-depending perturbation of an integrable system is the destruction of the invariant curves. For small perturbations many invariant curves subsist according to KAM theorem. An increase in the size of perturbations produces, eventually, the destruction of the curves. The stochastic zone is then very large.

In this paper we present for the standard map a geometrical approach to obtain values of the parameter for which no invariant curves exist. This is due to the existence of heteroclinic points. As it has been observed using other methods, there are several scaling properties in the phenomena which are also discussed here.

1. Introduction

In this paper we study the problem of existence of invariant curves (KAM curves) in area-preserving maps in the plane. The importance of this problem comes from the fact that the study of many 2 degree of freedom hamiltonian systems can be reduced to the study of diffeomorphisms on two-dimensional manifolds [1]. Such maps usually belong to a one-parameter family of diffeomorphisms on the annulus (or on the cylinder).

We study a one-parameter family of area-preserving maps known as standard maps [1, 2]. For small values of the parameter K, there are a lot of invariant rotational curves (IRC) on the cylinder [3]. Nevertheless there is some value of $K(K_c)$ for which all KAM curves disappear. Any invariant curve is destroyed for some critical value of K between 0 and K_c.

Mather [4] obtained a rigorous upper bound of K_c ($K_c < \frac{4}{3}$). This was found using the fact that any invariant curve of the twist map on the plane is the graph of a Lipschitz function. MacKay [5] refined this method and found a better upper bound ($K_c < \frac{63}{64}$) using the cone-crossing criterion.

Heuristic methods give better values of K_c. For instance, Greene [2] reached the most accurate value of K_c ($K_c = 0.971635406$) using the residue criterion. Greene conjectured that the loss of local stability of the elliptic periodic points close to an IRC is related to the destruction of this curve.

In this paper we show a new rigorous method to reach an upper bound of the critical value K_c of any IRC with quadratic irrational rotation number α. Moreover, this method gives rescaling relations related to the IRC. In fact the method given allows to obtain an upper bound of K_c for any irrational rotation number α.

The method is similar to the overlap criterion given by Chirikov [1]. The invariant manifolds of the hyperbolic periodic points (HPP) play the role of the separatrices. This method allows a relation between scaling for critical circles [12, 13] and the overlap criterion. The eigenvalues of HPP's show rescaling behavior like in the Greene method [2] but here the eigenvalues are related to the global behavior of the dynamics and not only to the local stability.

Although our method spends a lot of computer time, the numerical experiments show that it is

0167-2789/87/$03.50

possible to obtain recurrent rules that give the estimated value of K_c of any IRC with quadratic irrational rotation number.

2. Obstruction to invariant curves by heteroclinic tangencies

In this section we describe a method to find an upper bound of the critical value of the parameter (K_c) such that a specific IRC disappears.

Let f_K be a one-parameter family of area-preserving diffeomorphisms on the cylinder $\mathbb{S}^1 \times \mathbb{R}$, such that its lift on $\mathbb{R}^2$, F_K, has the form

$$F_K(x, y) = (x + y + g_K(x), y + g_K(x)),$$

where K is the parameter and $g_K(x)$ is a 1-periodic analitic function with zero average. It is clear that it has the twist property;

$$\frac{\partial}{\partial y} \Pi_1 F_K(x, y) > 0,$$

where Π_1 is the projection onto the first variable.

An IRC is the graph of a Lipschitz function, $y = \phi(x)$, which separates the cylinder in two invariant sets [2]. This curve has a rotation number (RN) defined as

$$\omega = \lim_{n \to \infty} \frac{\Pi_1 F_K^n(x, \phi(x)) - x}{n}.$$

Periodic orbits $\{x_n\}$ have a rational RN p/q where $\Pi_1 F^q(x, y) = x + p$ and $(x, y) \in \{x_n\}$. These periodic orbits are formed by hyperbolic, elliptic or parabolic points. When $K = 0$, the map is integrable and the orbits are IRC ($\omega \in \mathbb{R} \setminus \mathbb{Q}$) and parabolic periodic points ($\omega \in \mathbb{Q}$).

For any interval $[\omega_0, \omega_1]$ (where ω_0 and ω_1 are associated to some orbits in the cylinder) any $\omega \in [\omega_0, \omega_1]$ has associated an invariant set between the orbits with rotation number ω_0 and ω_1 [7]. If $\omega \in \mathbb{Q}$ the set contains periodic orbits (hyperbolic, elliptic or parabolic) with RN ω as well

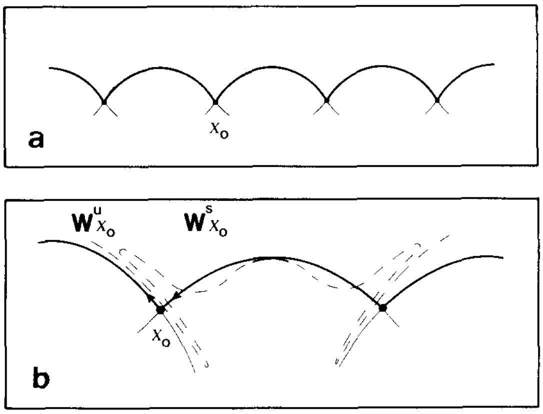

Fig. 1. a) $G\phi_{x_0}$ is the union of separatrices. b) $G\phi_{x_0}$ is composed by segments of the invariant manifolds of x_0.

as other points (e.g. the stable manifold of the HPP and the points which circulated around an elliptic point under F^q).

Lemma 1. Let x_0 and x_1 be two HPP of F_K, with rational RN ω_0 and ω_1. If the unstable invariant manifold ($W^u x_0$) of x_0 and the stable invariant manifold ($W^s x_1$) of x_1 have nonempty intersection (i.e. there exist heteroclinic points), then there is not an IRC with RN $\omega \in (\omega_0, \omega_1)$.

Proof. Assume that the invariant curve with RN $\omega_c \in (\omega_0, \omega_1)$ is the graph (on the lift) of the function $\phi_c(x)$. The graph of the function ϕ will be denoted by $G\phi$. Let $x_0 s x_1$ a continuous path that joints x_0, x_1 and the heteroclinic point s, formed by the union of one piece of $W^u x_0$ and one piece of $W^s x_1$. Due to the preservation of measure the point x_0 has homoclinic points. Either there exist a homoclinic connection (i.e. a separatrix) or it does not exist. In the first case we define ϕ_{x_0} such that $G\phi_{x_0}$ is the union of separatrices. In the second case $G\phi_{x_0}$ is composed by segments of $W^u x_0$ and $W^s x_0$. In any case we obtain a closed curve encircling the cylinder (fig. 1). ϕ_{x_1} is a similar function related to x_1.

It is clear that $G\phi_c \cup x_0 s x_1 = \varnothing$, $G\phi_c \cup G\phi_{x_0} = \varnothing$ and $G\phi_c \cup G\phi_{x_1} = \varnothing$. This implies that both $\phi_c(x) - \phi_{x_0}(x)$ and $\phi_c(x) - \phi_{x_1}(x)$ do not change sign. As $\omega_1 > \omega_c$ from $\Pi_1 F_K(x, \phi_{x_1}(x)) - \Pi_1 F_K(x, \phi_c(x)) = \phi_{x_1}(x) - \phi_c(x)$ it follows $\phi_{x_1}(x) - \phi_c(x) > 0$.

Similarly, we obtain $\phi_c(x) - \phi_{x_0}(x) > 0$. Hence $G\phi_c$ lies between $G\phi_{x_0}$ and $G\phi_{x_1}$. Therefore $x_0 s x_1$ should have non empty intersection with $G\phi_c$, which is an absurdity. □

Lemma 2. With the hypothesis of lemma 1, let x_2 and x_3 other HPP with RN ω_2, ω_3 such that $\omega_0 < \omega_2 < \omega_3 < \omega_1$. If x_0 and x_1 have heteroclinic points for the parameter value K_0, then x_2 and x_3 also have heteroclinic points.

Proof. $G\phi_{x_0}$ and $G\phi_{x_1}$ define, by lemma 1, an instability domain (there are not IRC [6]). Using the same construction of lemma 1 we get the continuous functions ϕ_{x_2}, ϕ_{x_3} of x_2 and x_3 respectively. For any x we get

$$\phi_{x_0}(x) < \phi_{x_2}(x) < \phi_{x_3}(x) < \phi_{x_1}(x).$$

Then ϕ_{x_2} and ϕ_{x_3} define an unstable domain. Let U_ε a disk of radius $\varepsilon > 0$ centered in x_2; then $\forall \varepsilon > 0$ $W^u x_2 \cap U_\varepsilon \neq \varnothing$. Let $V = \bigcup_{n \in \mathbb{Z}} F_K^n(U_\varepsilon)$. Using the remark 5.9.3 of [6], we have $\phi_{x_3} \cap V \neq \varnothing$ and as this is true for all $\varepsilon > 0$ we obtain $\phi_{x_3} \cap W^u x_2 \neq \varnothing$. Hence, $W^u x_2 \cap W^s x_3 \neq \varnothing$, that is x_2 and x_3 have heteroclinic points. □

Remark.

$$W^u x_0 \cap W^s x_2 \neq \varnothing \quad \text{and} \quad W^s x_1 \cap W^u x_2 \neq \varnothing.$$

Lemma 3. Let ω_n a sequence of rational numbers such that

i) $\omega_n = p_n/q_n$, $\quad q_n, p_n \in \mathbb{N}$,
ii) $\lim_{n \to \infty} \omega_n = \omega$,
iii) $|\omega - \omega_{n+1}| < |\omega - \omega_n|$,
iv) $(\omega - \omega_{n+1})(\omega - \omega_n) < 0$.

For any $n \in \mathbb{N}$ let x_n and x_{n+1} be HPP with RN ω_n, ω_{n+1} (respect.) and let us suppose that they do not have heteroclinic points for $K < K_n$ and they have such heteroclinic points for $K > K_n$. Then, for $m > n$ we have $K_m \le K_n$.

Proof. For every $K_1 \ge K \ge K_n$, x_m and x_{m+1} have heteroclinic points (lemma 2). Therefore $K_m \le K_n$. □

Corollary. The sequence K_n is decreasing,

$$K_1 \ge K_2 \ge \cdots \ge K_n \ge K_{n+1} \ge \cdots > 0.$$

In order to know the critical value of the parameter (K_c) for the IRC with RN ω, we can take the continued fraction expansion of ω [8],

$$\omega = [a_1, a_2, a_3, \ldots]$$
$$= 1/(a_1 + 1/(a_2 + 1/(a_3 + \cdots))).$$

We denote by ω_n the finite expansion $[a_1, a_2, \ldots, a_n]$.

Then we find the "first" heteroclinic tangency (i.e. a tangency which happens for some value $K = K_n$, and such that there are not heteroclinic points for $0 \le K \le K_n$) of the HPP with RN's ω_n and ω_{n+1}.

From lemma 3 and corollary 1 we obtain a decreasing sequence $\{K_n\}$ such that its limit is an upper bound of the K_c, that is there is not IRC of RN ω for $K = K_\infty = \lim_{n \to \infty} K_n$ and there are such curves for $0 < K < K_\infty$.

Obviously, it is impossible to detect the "first" heteroclinic tangency of two HPP because we should extend infinitely the invariant manifolds. In any way, we can fix a particular tangency that determines uniquely one value of the parameter $k_n \ge K_n$.

Definition 1. Let x_0 and x_1 HPP and $W^u x_0$ and $W^s x_1$ its invariant manifolds expanded in parametric form,

$$W^u x_0 = (\xi_0(s), \eta_0(s)), \qquad s, t \in \mathbb{R}^+ \cup \{0\},$$
$$W^s x_1 = (\xi_1(t), \eta_1(t)),$$

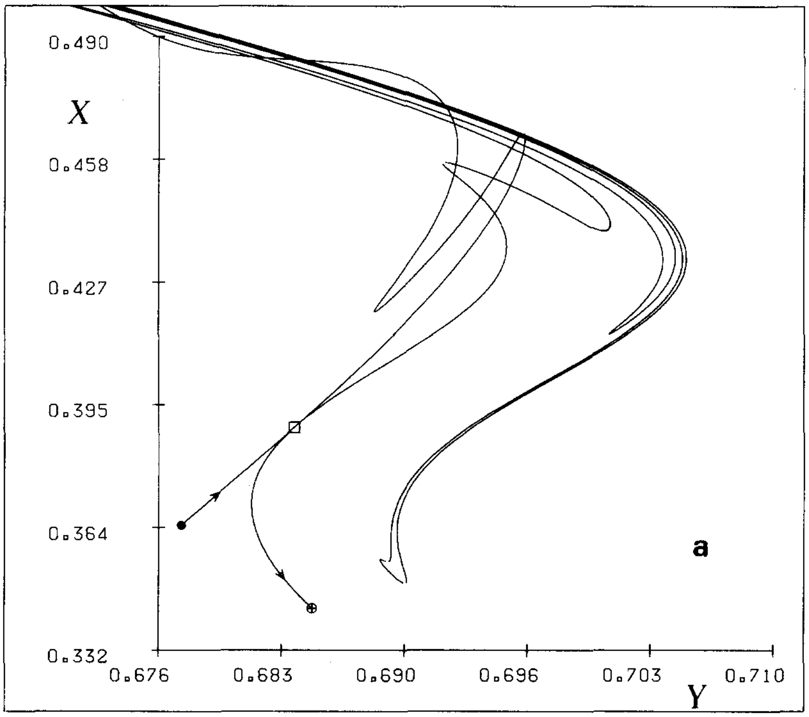

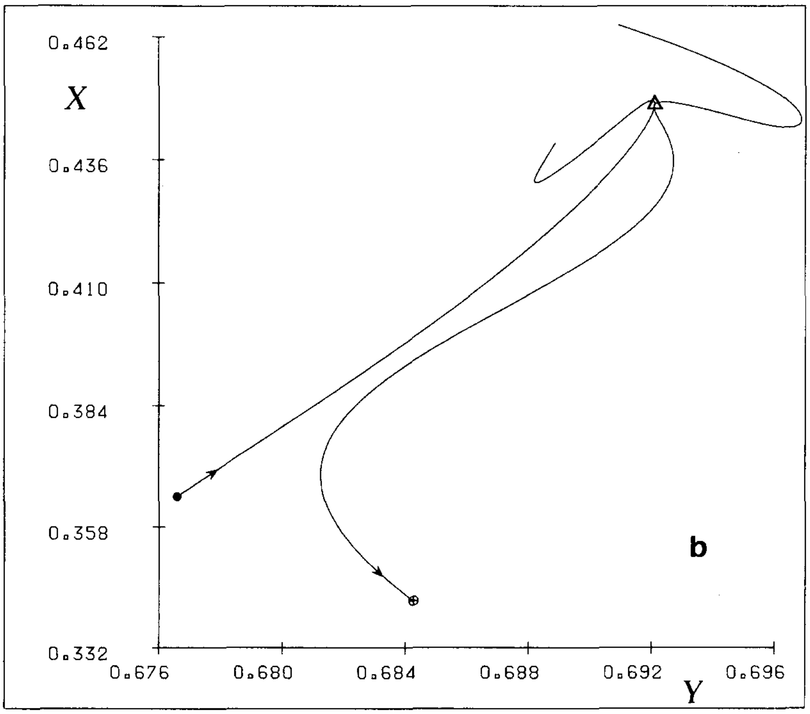

Fig. 2. a) The stable invariant manifold of the HPP with RN $\omega = \frac{5}{8}$ (⊕) has heteroclinic tangency (□) on the first tongue with the unstable invariant manifold of the HPP with RN $\omega = \frac{8}{13}$ (●) at the parameter value $K = 1.085169$. b) The same points have heteroclinic tangency (△) on the second tongue at the parameter value $K = 1.0547$.

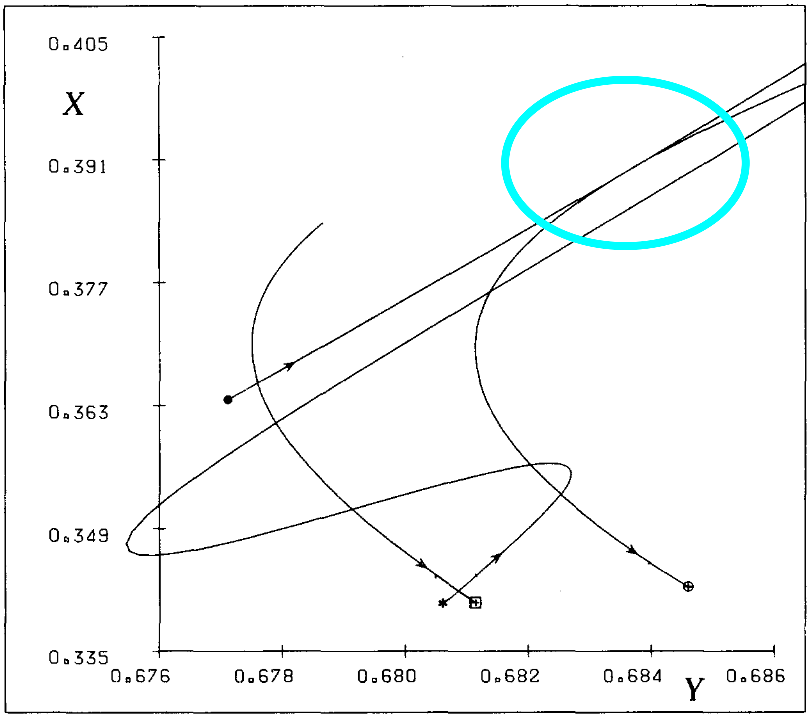

Fig. 3. The HPP's with RN $\omega = \frac{5}{8}$ (⊕) and $\omega = \frac{8}{13}$ (●) have heteroclinic tangency for $K = 1.085169$. HPP's with rotation numbers in the interval $[\frac{5}{8}, \frac{8}{13}]$ have transversal intersections between their invariant manifolds; in this case $\omega = \frac{13}{21}$ (⊞) and $\omega = \frac{21}{34}$ (*) do it.

such that $(\xi_0(0), \eta_0(0)) = \boldsymbol{x}_0$ and $(\xi_1(0), \eta_1(0)) = \boldsymbol{x}_1$.

We call heteroclinic tangency on the "first tongue" a tangency which happens for values of t and s such that

i) $(\xi_0(s_0), \eta_0(s_0)) = (\xi_1(t_0), \eta_1(t_0))$;

ii) $((\mathrm{d}/\mathrm{d}s)\xi_0(s_0), (\mathrm{d}/\mathrm{d}s)\eta_0(s_0)) \cdot ((\mathrm{d}/\mathrm{d}t)\eta_1(t_0), -(\mathrm{d}/\mathrm{d}t)\xi_1(t_0)) = 0$, where $\cdot$ denotes the scalar product;

iii) The curvature of $W^{\mathrm{u}}\boldsymbol{x}_0$ (resp. $W^{\mathrm{s}}\boldsymbol{x}_1$) for $0 < t \le t_0$ (resp. $0 < s \le s_0$) have the same sign.

We take as k_n the minimal value of K for which i), ii) and iii) hold.

The fig. 2a shows the heteroclinic tangency on the first tongue while fig. 2b shows the tangency on the second tongue.

Remark. Generically, if $\boldsymbol{x}_0$ and $\boldsymbol{x}_1$ are HPP and have heteroclinic tangency on the first tongue for k_0, there exists $\delta > 0$ such that $W^{\mathrm{s}}\boldsymbol{x}_0 \pitchfork W^{\mathrm{u}}\boldsymbol{x}_1 \neq \varnothing$ (where $\pitchfork$ denotes transversal intersection as usual) for values of K such that $|k_0 - K| > \delta$. Furthermore $\boldsymbol{x}_0$ and $\boldsymbol{x}_1$ have homoclinic points. Then tongues of higher order intersect every neighbourhood of the tangency points of $W^{\mathrm{s}}\boldsymbol{x}_0$ and $W^{\mathrm{s}}\boldsymbol{x}_1$.

Let k_n the value of the parameter related to the HPP $\boldsymbol{x}_n$ and $\boldsymbol{x}_{n+1}$ with RN ω_n and ω_{n+1} as defined above. In spite of the fact that the heteroclinic tangency of the "first tongue" is not the "first" tangency, we conjecture that the sequence $\{k_n\}$ is strictly decreasing. We note that even if the sequence $\{k_n\}$ is not decreasing we should have $\inf K_n \le \inf k_n$.

Fig. 3 shows the heteroclinic tangency on the "first tongue" of points with RN $\omega_5 = \frac{5}{8}$ and $\omega_6 = \frac{8}{13}$. The points with $\omega_7 = \frac{13}{21}$ and $\omega_8 = \frac{21}{34}$ have had heteroclinic tangency on the "first tongue" for a value of $K < k_5$. Numerical results show that this conjecture is true for different IRC.

3. Numerical method

In this section we describe the numerical method for the computation of heteroclinic tangencies. In order to find the K_c of some IRC we follow the steps: a) To find the HPP with RN ω_n and ω_{n+1}; b) to expand locally and analytically the invariant manifolds of these points; c) to continue numerically the invariant manifolds as far as required; d) to determine the distance between the manifolds in order to find the tangency. Then, repeating these steps for better approximations of ω by ω_n and ω_{n+1}, we obtain the sequence of $\{k_n\}$.

We give a short description of the steps:

a) *Periodic points.* Given a rational number $\omega_n = p_n/q_n$ and K, to find a HPP having this RN is not difficult. Every periodic orbit has two points belonging to the symmetry lines of the map [2] ($x = 0$, $x = \frac{1}{2}$, $x = y/2$ and $x = (y+1)/2$). Then this reduces the problem of finding a fixed point of F^q in the plane to an 1-dimensional problem. When the family of periodic orbits of period q_n is obtained we select the ones with RN ω_n and hyperbolic eigenvalues.

b) *Invariant manifolds.* To obtain a piece of an invariant manifold of HPP of high period by iteration of points of its linear approximation requires a lot of computation time. It is necessary to get a better approximation, that is, a degree-m polynomial approximation of the invariant manifold $y = \phi(x)$,

$$y = \phi_m(x) = y_0 + \sum_{i=1}^{m} a_i (x - x_0)^i,$$

where (x_0, y_0) is the HPP. To obtain the function ϕ we apply the definition of invariant set,

$$\Pi_2 f^q(x, \phi(x)) = \phi(\Pi_1 f^q(x, \phi(x))), \tag{1}$$

where f^q is the composition of the map f q-times. The map f^q can be represented by its Taylor series of order m,

$$\Pi_r f_m^q(x, y) = \sum_{i+j \le m} \frac{1}{i!\,j!} \frac{\partial^{i+j}}{\partial x^i \partial y^j} \times (\Pi_r f^q(x_0, y_0))(x - x_0)^i (y - y_0)^j, \tag{2}$$

where $r = 1, 2$. The partial derivatives are obtained in a recurrent way [14].

Replacing f^q and ϕ by their approximations (f_m^q and ϕ_m) in (1), it is possible to write (1) as a polynomial in x.

Equating the terms with the same power of x we get $m - 1$ relations [14] from which a_j is determined as a function of a_i, $i = 1, \ldots, j-1$.

c) *Continuation of the manifold.* In the invariant manifold we choose an interval of x defined as

$$[\Pi_1 f^{\pm q}(x_0 + \varepsilon, \phi(x_0 + \varepsilon)), x_0 + \varepsilon],$$

where $(+)$ is used for the stable manifold and $(-)$ for the unstable manifold. Then by iteration of points on this interval we can follow the invariant manifold until the sign of the curvature changes (this means that we have expanded the "first tongue" of the invariant manifold). Finally we can interpolate the invariant manifold using, for instance a cubic spline to get a smooth curve.

d) *Distance between manifolds.* When the invariant manifolds of suitable HPP with RN's ω_n and ω_{n+1} are available, we measure the signed distance between them taking intervals of y such that the first tongues of $\boldsymbol{W}^u \boldsymbol{x}_n$ and $\boldsymbol{W}^s \boldsymbol{x}_{n+1}$ are defined (in each interval) by a cubic approximation. Then we look for the minimum of the difference between them.

e) *Loop.* For each value of K we obtain some distance between the manifolds. Hence we have a function from $\mathbb{R}$ to $\mathbb{R}$ and its zero means the heteroclinic tangency of the "first tongue". Using a secant method [11] we determine numerically the zero of the function and we call it k_n.

f) *Sequence*. Applying the above method for each pair of HPP with RN ω_n and ω_{n+1}, $n = 1, 2, 3, \ldots$, we obtain the sequence $\{k_n\}$.

4. Numerical results

It is interesting to study some particular IRC because they seem to be the last broken curves in a given annulus. They are those whose continued fractions have only ones in the tail; we call them golden curves. In particular, a curve whose RN is the golden mean $(\sqrt{5}-1)/2 = 0.61803..$ seems to be the last IRC which disappears for the standard map.

In this section we show numerical experiments with golden curves. We found their K_c and geometrical properties of $\{k_n\}$. Moreover, a relation of the residues and the rotation numbers is found. Other kinds of curves were investigated too, those whose continued fraction expansion (CFE) is composed by the same integer (2 or 3) and those whose CFE has a periodic sequence of integers.

We have used quadruple precision arithmetic (32 significant figures) in order to obtain the position of the HPP with an error less than 10^{-27} and the invariant manifolds are computed with a similar error on the first tongue.

In order to optimize the computer time, we set the polynomial degree of the invariant manifolds of the HPP equal to 4 and we choose suitable error bounding in order to get spline approximation better than 10^{-15}.

4.1. *Golden mean circle*

The numerical experiment was done taking the RN of the IRC equal to the golden mean. Its CFE has only ones ($[1,1,1,\ldots]$). Hence, the sequence of rational RN obtained by truncation of the expansion is given by the Fibonacci numbers.

We have obtained the numerical value of k_n from $n = 2$ to 15. Table I shows the first values of the sequence. It looks like a geometrical sequence such that its ratio defined as

$$\delta_n = \frac{k_{n+1} - k_n}{k_n - k_{n-1}}$$

goes to a constant value as n grows (table I shows this sequence of δ_n). Keeping the last value of δ_n fixed as δ_∞, we can estimate the value of $k_\infty \approx 0.971636$. This value is similar to Greene critical value of K. Moreover the value of δ_n is close to the golden mean (ω_g),

$$\frac{\delta_n}{\omega_g} \approx 0.99448.$$

Table I
Sequence $1,1,1,1,1,\ldots$

n	ω_n	ω_{n+1}	k_n	δ_n	$R_{n,n}$	$R_{n,n+1}$
2	2/3	3/5	1.326626		−0.694465	−1.266627
3	3/5	5/8	1.165048		−0.635144	−1.208576
4	5/8	8/13	1.085169	0.494391	−0.658421	−1.160677
5	8/13	13/21	1.040234	0.562529	−0.641524	−1.194757
6	13/21	21/34	1.013046	0.605046	−0.653180	−1.172093
7	21/34	34/55	0.996923	0.593061	−0.645622	−1.186590
8	34/55	55/89	0.987076	0.612808	−0.650782	−1.178554
9	55/89	89/144	0.981093	0.606031	−0.647420	−1.183125
10	89/144	144/233	0.977430	0.613199	−0.649274	−1.179617
11	144/233	233/377	0.975192	0.611134	−0.648131	−1.181773
12	233/377	377/610	0.973818	0.613869	−0.648833	−1.180450
13	377/610	610/987	0.972975	0.613086	−0.648403	−1.181260
14	610/987	987/1597	0.972458	0.614116	−0.648666	−1.180764
15	987/1597	1597/2584	0.972140	0.613818	−0.648505	−1.181067

Following Greene we defined the residue of a HPP with eigenvalues λ and λ^{-1} as $R=(2-\lambda-\lambda^{-1})/4$. Let us denote by $R_{n,n}$ the residue of the HPP with RN ω_n for $K=k_n$, and $R_{n,n+1}$ the corresponding residue for the orbit related to ω_{n+1} for $K=k_n$. It has been observed that $R_{n,n}$ goes to a limit value when n goes to infinity and the same is true for $R_{n,n+1}$ (see table I). Let S_n defined as $S_n=R_{n,n}/R_{n,n+1}$. It follows that S_n has a limit S_∞ for $n\to\infty$ and furthermore S_∞ (in this case $S_\infty=0.549..$) is not far from ω_g. Moreover, S_n converges geometrically. This behavior shows that the heteroclinic tangency can be rescaled to a universal map, where the tangency (or the overlap of the separatrices) occurs when the residues ratio has a value close to the RN.

We must remark that in table I (and the following ones) only 6 figures are given for the value of k_n. As we stated before all the computations were done in quadruple precision. For instance for $n=13$ the value of k_{13} is close to 0.9729758998045303. If only 6 figures are taken for high periods, we are relatively far from the heteroclinic tangency and, the residues change very much because of their sensitivity to the value of K. For instance for k_{13} we have $R_{13,14}=-1.181260$, while if the value $K=0.972976$ is taken we have the residue $R=-1.181398$.

4.2. *Other golden circles*

In order to investigate how the tail of the CFE drives the behavior of $\{k_n\}$ and their residues, we studied three IRC whose RN have CFE equal to ω_g except in the first term, that is

$$\omega_{g_q}=[q,1,1,1,1,\dots],\quad \text{with } q=3,5,7.$$

As in 4.1, we obtained sequences $\{k_n\}$ and the respective residues for each ω_{g_q}. They are shown in fig. 4. As in the previous case, the value of δ_n converges close to ω_g when n grows (see fig. 4).

We conclude that golden circles are rescaled to one universal map for which the global behavior of the invariant manifolds and its eigenvalues is unique.

4.3. *Non-golden circles*

The next question to study is the behavior of the different magnitudes so far introduced when the RN has a CFE with all the quotients equal but different from 1.

For circles with RN $\omega_2=[2,2,2,2,\dots]=\sqrt{2}-1=0.414213..$ and $\omega_3=[3,3,3,3,\dots]=(\sqrt{13}-2)/2=0.30277..$ we obtain sequences $\{k_n\}$ and their respectives residues. They are shown in tables II and III. As in the golden case, the rescaling parameter δ_n converges to a value close to the RN (0.4087 for ω_2 and 0.2951 for ω_3). Keeping the last value of δ_n fixed we obtain the critical value for these curves:

$$\omega_2\to k_\infty\approx 0.957447,$$
$$\omega_3\to k_\infty\approx 0.892257.$$

The behavior of the residue as in the previous cases shows a fast convergence to a fixed value such that its ratio S_n is not far from the RN,

$$\omega_2\to S_n\approx 0.347820,$$
$$\omega_3\to S_n\approx 0.251971.$$

4.4. *Periodic expansions*

Finally we studied circles whose RN have CFE with period $(a_1,a_2,a_3,\dots,a_m)$ such that its RN is $\omega=[a_1,a_2,\dots,a_m,a_1,a_2,\dots]=[(a_1,a_2,\dots,a_m)^\infty]$. We choose the periods (2,1) (3,1), (3,2) and (2,1,1) in order to verify if these circles share the behavior of the previous cases. Repeating the same numerical analysis the results are shown in table IV. We can see that the sequence of the residue values have as many accumulation points as the length of the period. Then, instead of computing the rescaling parameter δ_n like above we take the relation

$$\delta_n^i=\frac{k_{n+i}-k_n}{k_n-k_{n-i}},\quad i=\text{length of the period}.$$

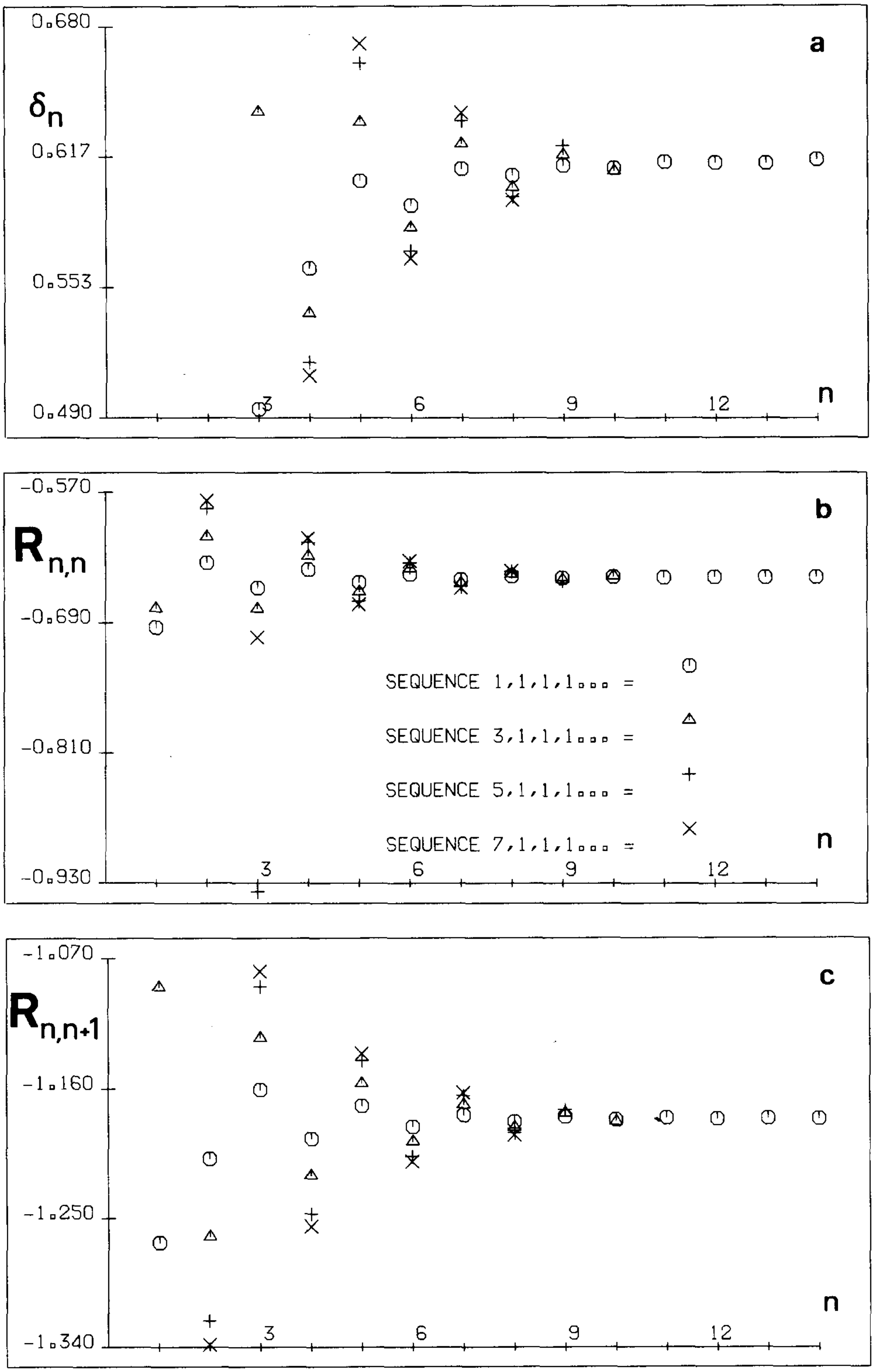

Fig. 4. a) The scaling parameter δ_n versus n is shown for four golden circles. The behavior of the residues $R_{n,n}$ and $R_{n,n+1}$ as function of n are shown in b) and c) for the same golden circles.

Table II
Sequence 2, 2, 2, 2, 2, ...

n	ω_n	ω_{n+1}	k_n	δ_n	$R_{n,n}$	$R_{n,n+1}$
2	2/5	5/12	1.100098		−0.470191	−1.375662
3	5/12	12/29	1.011318		−0.475989	−1.354572
4	12/29	29/70	0.979939	0.353459	−0.472700	−1.365228
5	29/70	70/169	0.966585	0.425556	−0.474226	−1.360535
6	70/169	169/408	0.961179	0.404785	−0.473580	−1.362493
7	169/408	408/985	0.958972	0.408260	−0.473846	−1.361690
8	408/985	985/2378	0.958070	0.408770	−0.473737	−1.362014

Table III
Sequence 3, 3, 3, 3, ...

n	ω_n	ω_{n+1}	k_n	δ_n	$R_{n,n}$	$R_{n,n+1}$
1	1/3	3/10	1.073727		−0.360927	−1.456069
2	3/10	10/33	0.941849		−0.365146	−1.446520
3	10/33	33/109	0.905810	0.273281	−0.364994	−1.446497
4	33/109	109/360	0.895306	0.291782	−0.364953	−1.446715
5	109/360	360/1189	0.892190	0.295135	−0.365161	−1.449215

Table IVA
Sequence 2, 1, 2, 1, 2, 1, ...

n	ω_n	ω_{n+1}	k_n	δ_n^2	$R_{n,n}$	$R_{n,n+1}$
3	3/8	4/11	1.080201		−0.633317	−1.236220
4	4/11	11/30	0.996771		−0.488494	−1.230738
5	11/30	15/41	0.975805		−0.617239	−1.271063
6	15/41	41/122	0.954894		−0.495081	−1.213848
7	41/112	56/153	0.949580	0.251215	−0.612207	−1.280731
8	56/153	153/418	0.944127	0.257130	−0.496996	−1.209315
9	153/418	209/571	0.942737	0.260919	−0.611170	−1.284093
10	209/571	571/1560	0.941298	0.262670	−0.497501	−1.208159

Table IVB
Sequence 3, 2, 3, 2, 3, 2, ...

n	ω_n	ω_{n+1}	k_n	δ_n^2	$R_{n,n}$	$R_{n,n+1}$
2	2/7	7/24	0.968055		−0.380360	−1.360852
3	7/24	16/55	0.927112		−0.450009	−1.464424
4	16/55	55/189	0.906459		−0.383909	−1.350152
5	55/189	126/433	0.901619		−0.448459	−1.472233
6	126/433	433/1488	0.899087	0.122763	−0.384232	−1.345957
7	433/1488	992/3409	0.898489	0.119685	−0.448036	−1.471389

Table IVC
Sequence 3, 1, 3, 1, 3, 1, ...

n	ω_n	ω_{n+1}	k_n	δ_n^2	$R_{n,n}$	$R_{n,n+1}$
1	1/3	1/4	1.289159		−0.635263	−1.221281
2	1/4	4/15	0.971240		−0.383228	−1.276322
3	4/15	5/19	0.925345		−0.597572	−1.293614
4	5/19	19/72	0.870134		−0.394593	−1.236420
5	19/72	24/91	0.861546	0.175362	−0.586974	−1.317640
6	24/91	91/345	0.850432	0.194869	−0.397675	−1.228016
7	91/345	115/436	0.848680	0.201661	−0.584905	−1.323665
8	115/436	436/1653	0.846378	0.205749	−0.398300	−1.226453

Table IVD
Sequence 2, 1, 1, 2, 1, 1, ...

n	ω_n	ω_{n+1}	k_n	δ_n^3	$R_{n,n}$	$R_{n,n+1}$
2	1/3	2/5	1.302717		−0.656262	−1.148995
3	2/5	5/13	1.096353		−0.461895	−1.342430
4	5/13	7/18	1.041419		−0.651754	−1.202505
5	7/18	12/31	1.009960		−0.667858	−1.117147
6	12/31	31/80	0.983275		−0.454372	−1.371805
7	31/80	43/111	0.975183		−0.659711	−1.186312
8	43/111	74/191	0.970501		−0.662477	−1.126748
9	74/191	191/493	0.966364		−0.456155	−1.366039
10	191/493	265/684	0.965101	0.149548	−0.658234	−1.189030
11	265/684	456/1177	0.964362	0.155556	−0.663407	−1.125146

Obviously we have two (or three) sequences of δ_n^i for each circle but the limits of these sequences are the same (see tables IVA–D).

If the RN has periodic expansion $(a_1, a_2, \ldots, a_m)$ then the limit of the δ_n^i seems to be close to $\omega_{a_1}\omega_{a_2}\cdots\omega_{a_m}$ (where $\omega_{a_i} = [(a_i)^\infty]$):

Period (2, 1)

$$\delta_n^2 = 0.262670 \sim \omega_2\omega_1 = 0.2560\ldots,$$

Period (3, 1)

$$\delta_n^2 = 0.205749 \sim \omega_3\omega_1 = 0.1871\ldots,$$

Period (3, 2)

$$\delta_n^2 = 0.119685 \sim \omega_3\omega_2 = 0.1254\ldots,$$

Period (2, 1, 1)

$$\delta_n^3 = 0.155556 \sim \omega_2\omega_1\omega_1 = 0.1582\ldots.$$

5. Conclusion

We have given a rigorous method to find an accurate lower bound of K_c such that there is not an IRC with RN ω by using the heteroclinic tangency of the invariant manifolds. This method is rigorous because each element of the sequence $\{k_n\}$ assures the non-existence of the IRC, similar to the cone-crossing criterion [5] but with precision of the residue method [2].

The idea of the method is similar to the Chirikov's overlap criterion [1] applied to diffeomorphisms.

The method shows geometrical behavior of the sequence $\{k_n\}$. The limit of the value of its rescaling parameter δ_n (or δ_n^i) is close to the RN of the invariant circle (but not equal). If we use higher order tongues of the invariant manifold to find the heteroclinic tangency we will obtain better upper bounds of k_n and the difference between δ_n and ω could be less than the actual value. Nevertheless it is difficult to detect tangencies of higher order tongues.

The heteroclinic tangency of the invariant manifolds could explain the existence of a narrow channel allowing for transport across the destroyed IRC [10].

This method spends a lot of computer time but knowing only the value of k_n for a number of cases equal to the double of the period of the CFE of ω we can estimate k_∞.

Acknowledgements

This work has been possible thanks to a Grant from CONACYT (México) to the first author. The work of the second author has been supported by CAICYT Grant 3534/83C3 (Spain). The computer facilities of the University of Barcelona were used.

References

[1] B.V. Chirikov, Phys. Reports 52 (1979) 263.
[2] J.M. Greene, J. Math. Phys. 20 (1979) 1183.
[3] H. Russmann, Lect. Notes in Maths. 1007 (1983) 677.
[4] J.N. Mather, Erg. Theory & Dyn. Syst. 4 (1984) 301.
[5] R.S. MacKay and I.C. Percival, Converse KAM: Theory and Practice, preprint (1984).
[6] M.R. Herman, Astérisque 103–104 (1983).
[7] J.N. Mather, Topology 21 (1982) 457.
[8] A.Ya. Khintchine, Continued Fractions (Noordhoff, Groningen, 1963).
[9] M. Abramowitz and I. Stegun, Handbook of Mathematical Functions (Dover, New York, 1972).
[10] I. Dana and S. Fishman, Physica 17D (1985) 63.
[11] G. Dahlquist and Å. Bjorck, Numerical Methods (Prentice-Hall, New York, 1969).
[12] S.J. Shenker and L.P. Kadanoff, J. Stat. Phys. 27 (1982) 631.
[13] R.S. MacKay, Renormalisation in Area Preserving Maps, Thesis, Princeton 1982 (Univ. Microfilms Int., Ann Arbor MI).
[14] A. Olvera and C. Simó, "Heteroclinic Tangencies on the Standard Map", Communication to the VIII Congreso de Ecuaciones Differenciales y Aplicaciones, Santander, Spain (1985).